Silane Functionalized Ethylene/Diene Copolymer Modifiers in Composites of Heterophasic Polypropylene and Microsilica

S. Lipponen[1], P. Pietikäinen[1], U. Vainio[2], R. Serimaa[2] and J.V. Seppälä[1]*

[1]Helsinki University of Technology, Department of Chemical Technology, P.O. Box 6100, FI-02015 TKK, Finland
[2]University of Helsinki, Division of X-Ray Physics, Department of Physical Science, P.O. Box 64, FI-00014, Finland

SUMMARY

Ethylene/1,7-octadiene copolymer was polymerised with metallocene catalyst and hydrosilylated to form silane functionalised polyethylenes (PE-co-SiX, X=Cl, OEt, Ph). The functionalised species were tested as modifiers in composites of rubber toughened polypropylene (heterophasic PP, hPP) and microsilica filler (µSi). A metallocene-based functionalised PE (PE-co-SiF) produced earlier in our laboratory and three commercial grades of functionalised polyolefins (one PE- and two PP-based) were used as reference modifiers. Major differences were seen in the toughness of the composites both above and below the glass transition temperature (T_g) of PP. In addition to increasing the stiffness, the microsilica filler enhanced the toughness of the heterophasic polypropylene by over 200% at ambient temperature. Below the T_g of PP (at -20 °C), the influence of µSi was the opposite and the impact strength of the hPP/µSi composite was below that of unfilled hPP. With the addition of just 2 wt% of functionalised polyethylene, the poor cold toughness of hPP/µSi composite was improved by nearly 100%. With the same addition, the toughness of the composites at ambient temperature was improved by 50 to 100% compared with the unfilled hPP. This behaviour was explained by significant changes in the fracture mechanism. Addition of functionalised PE increased the concentration of microsilica in the rubbery phase, allowing the crack to enter that phase. The rubbery phase was also able to absorb a large amount of impact energy below the glass transition temperature of PP.

INTRODUCTION

Polypropylene (PP) is a widely used and affordable polymer with excellent chemical resistance and processability and good mechanical properties. In fact, its mechanical property profile is close to that of some engineering thermoplastics. Its usefulness in engineering applications, as in the automotive industry, is limited, however, by its relatively poor impact resistance. The toughness of PP can be improved, at the cost of stiffness, by blending in rubber particles. Although the stiffness can be enhanced by embedding filler particles in the polymer matrix, the filler usually decreases the impact strength[1].

The phase structure in ternary PP/elastomer/filler composites can vary widely, and methods to increase stiffness and toughness simultaneously have generated much interest. Usually, these composites are divided into two classes according to their morphology. Either the filler and the elastomer are dispersed separately in the matrix, or the filler particles are embedded in the elastomeric phase (core-shell structure). In practice, the phase structure lies somewhere between these two morphologies, and a separated structure is obtained only when one of the phases in the composite contains some functionality. Functionalised polypropylene can be used as an adhesive to attach the filler to the

PP matrix, preventing the filler from dispersing into the rubbery phase[2]. A functionalised rubbery phase (e.g. EPR-g-MAH), in turn, favours the core-shell structure[3].

In some earlier studies it was concluded that the increase in toughness and decrease in stiffness could be correlated with the core-shell structure[3,4], although contrary results have also been reported[5]. Still today, the stiffness of ternary blends is considered to depend primarily on the amount of core-shell structure, even though the correlation between the toughness of a polyolefin-based composite and its morphology is known to be much more complex. As an extension of the idea of a core-shell structure, the toughness of a composite might be correlated with the interaction between the filler and the matrix. Recent studies have shown that fillers can act as toughening agents in the polypropylene matrix[1,6,7,8]. According

*Corresponding author. Tel.: +358-9-4512614; fax: +358-9-4512622.
E-mail address: jukka.deppala@tkk.fi

S. Lipponen, P. Pietikäinen, U. Vainio, R. Serimaa and J.V. Seppälä

to the common understanding, the filler separation from the matrix is the crucial factor in this filler toughening mechanism. In addition to the impact energy that is consumed when the filler is debonded from the matrix, the debonding process creates voids, and in some cases these voids can mimic a rubber toughening mechanism.

In addition to filler/matrix interaction, the size, shape, and quality of the filler and the microstructure of the matrix at the boundary layers between different phases can all influence the toughness of composites[1,7,9,10]. Basically, the crucial factors determining toughness are the prevailing micromechanical energy-consuming deformation process and the volume of this deformation.

Polyolefins modified by the introduction of polar groups have significant potential as adhesives and compatibilisers in film, fibre, and composite applications. Various synthetic strategies have been reported, including the direct copolymerisation of ethylene or propylene and functionalised monomers with co-ordination catalysts[11]. However, the sensitivity of the polymerisation catalyst toward nitrogen and oxygen donor atoms severely limits catalyst activity and co-monomer incorporation rates. This drawback can be avoided by post-functionalisation of unsaturated polymers prepared with metallocene catalysts[12]. Copolymerisation of α,ω-dienes provides an effective way to modify the structures of polyethylene[13,14,15] and polypropylene[16]. Functionalised polyolefins can then readily be obtained by subsequent reaction of the olefin unsaturation.

In this study, ethylene/1,7-octadiene copolymers were prepared with metallocene catalysts, and their terminal vinyl groups were functionalised via hydrosilylation reactions (**Figure 1**). These silane functionalised polyethylenes were used as modifiers in composites of rubber-modified PP (heterophasic

polypropylene, hPP) and microsilica (μSi). The goal was to control the filler concentration in the rubbery phase and the filler/matrix interaction, and thereby obtain a fuller understanding of the toughening mechanism in ternary PP/rubber/filler composites. In addition to the chemical structure of the synthesised copolymers, the thermal, morphological, crystalline, and mechanical properties of the composites were investigated.

EXPERIMENTAL

Materials

The catalyst, *rac*-ethylenebis (indenyl)zirconium dichloride (Et(Ind)$_2$ZrCl$_2$), and the co-catalyst, methylaluminoxane (MAO), were obtained from Witco GmbH and used without further purification. Ethylene (grade 3.5) was supplied by Oy AGA Ab, toluene (pro analysis) by Merck KGaA, and 1,7-octadiene (98%) by Sigma-Aldrich. Ethylene and toluene were purified by passing them through columns containing molecular sieves, Al$_2$O$_3$, and CuO. 1,7-Octadiene was dried with molecular sieves. Dimethylphenylsilane (>97%, b.pt. 156-157 °C),

dimethylethoxysilane (>97%, b.pt. 54-55 °C) and chlorodimethylsilane (b.pt. 36 °C) were from ABCR. The hydrosilylation catalyst (H$_2$PtCl$_6$) was from Sigma. Metallocene-based dimethylfluorosilane functionalised polyethylene (PE-*co*-SiF) was produced earlier in our laboratory[17]. The heterophasic polypropylene, grade 245 MO (PP/PP-*co*-PE, 16% of PP-*co*-PE; MFR 3.5 g/10 min, 230 °C/2.16 kg; containing nucleating agents), was supplied by Borealis Polymers Oy. Amorphous uncoated microsilica was from Elkem Materials, grade MS 983, with an average spherical particle size of 0.15 μm and density of 2.2-2.3 g/cm^3. The commercial grade functional polyolefins were Lotader 8840 (PE-*co*-GMA, glycidylmethacrylate 8 wt%) from Atofina, PolyBond 1002 (PP-*g*-COOH, acrylic acid 6 wt%) from Uniroyal Chemicals, and BB127E (PP-*g*-MAH, maleic acid anhydride 1 wt%) from Borealis Polymers Oy.

Polymerisation

Polymerisation reactions were carried out in a 0.5 dm^3 stainless steel Büchi autoclave. After careful evacuation of the reactor, toluene, MAO, and diene were introduced under vacuum and

Figure 1. Synthesized polyethylene/silane additives (PE-co-SiX), X=Cl, OEt, Ph
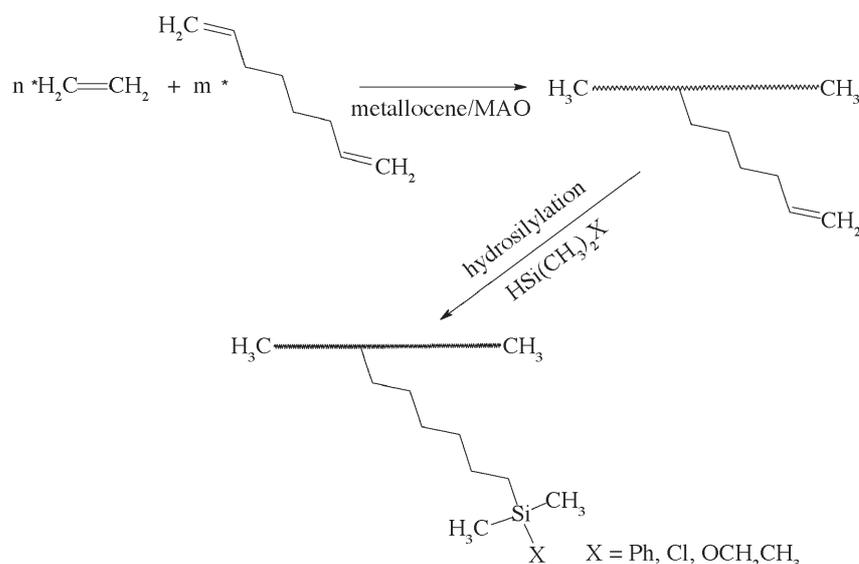
the reactor was filled with nitrogen to ambient pressure. Ethylene was then fed, and the pressure in the gas phase was adjusted. Finally, after the ethylene concentration in the reactor had reached equilibrium, the catalyst was fed to the reactor. The ethylene concentration in the polymerisation medium was kept constant during the polymerisation by continuous feeding and vigorous stirring. Polymerisations were stopped by degassing the reactor, and the reaction mixture was poured into a HCl/ethanol solution. After overnight stirring, the polymer was filtered out, washed with ethanol, filtered again, and dried.

Hydrosilylation

The post-treatments were conducted in a twin-necked 50 ml round bottom flask with a magnetic stirrer and a condenser. The untreated copolymer (~1 g, unreacted double bond 0.33 mmol) was added to the vessel after the vessel had been evacuated. Dry toluene (25 ml) was injected with a syringe through a silicone rubber septum and the stirred suspension was heated up to 100 °C enabling the copolymer to dissolve in the medium. The solution was cooled down to 25 °C and hydrosilane (~3.3 mmol, $HSi(CH_3)_2OEt$, $HSi(CH_3)_2Cl$, or $HSi(CH_3)_2Ph$) and the catalyst (0.05 ml 0.2 M H_2PtCl_6 in ethanol) were added. The solution was reheated to 100 °C and the reaction was allowed to continue for 4 h. The solution was cooled down to 25 °C, filtered and flushed with dry toluene in a glove box and finally dried in vacuum (70 °C) for one day.

Preparation of Composites

Heterophasic polypropylene (hPP) and microsilica (µSi) (70/30 wt%) were premixed by melt blending in a Brabender Plasti-Corder PLE 651 with a DSK 42/7 twin-screw extruder. The blending temperature was 200 °C and the screw speed 60 rpm (mean delay time of the extrudate 250 s.). The final composite was prepared by blending the polyolefin-based functionalized modifier (0.5 or 2.0 wt%) into the palletised premixed hPP/µSi extrudate in a twin-screw midi-extruder (DSM, speed 75 rpm, capacity 16 cm³, length 150 mm). After mixing for 5 min the blend was injection moulded into tensile and impact test specimens. The temperatures during blending and in injection moulding were 210 °C for tensile test specimens and 200 °C for impact test specimens. With a few exceptions, the mould temperature was 40 °C for both specimens. To obtain a fuller understanding of the fracture mechanism, the impact tests were also done on composites containing 1 wt% of functionalized polyethylene.

Characterisation

The melting temperatures and enthalpies of polymers and composites were measured with a Mettler Toledo DSC 821ᵉ differential scanning calorimeter. To achieve better contact between the sample and the aluminium sample pan, the sample (composite ~7.5 ± 1.0 mg, polymer ~5.0 ± 0.3 mg) was pre-melted in the pan (on a heated plate, 200 °C) at the same time as it was pressed firmly on the bottom of the pan. Before the non-isothermal runs the thermal history of the material was destroyed by heating the sample to 220 °C (PE-based copolymers to 160 °C) at 20 °C/min and holding it there for one minute. The crystallisation behaviour of the samples was then determined from the peak area and the peak temperature of the crystallisation exotherm (T_c), obtained at a cooling rate of 10 °C/min (from 220 °C to 0 °C). After the cooling step, the melting endotherms (ΔH) and the peak melting temperatures (T_m) were measured by reheating the sample at 10 °C/min.

The molar masses (M_w) and molar mass distributions (M_w/M_n) were determined with a Waters Alliance GPCV 2000 gel permeation chromatograph equipped with four Waters Styragel columns (HMW 7, 2*HMW 6, HMW 2) and a refractive index detector. 1,2,4-Trichlorobenzene was used as a solvent at 140 °C and applied at a flow rate of 1.0 ml/min.

The diene conversion and the conversions of the post-treatment reactions were determined from NMR spectra run with a Varian Gemini 2000 300-MHz NMR spectrometer. The copolymers were dissolved in 1,1,2,2-tetrachloroethane-d₂ (dried with molecular sieves), and the NMR spectra were recorded at 110 °C. As an internal standard, the resonance peak of the $C_2D\underline{H}Cl_4$ residue was placed at δ 5.9 ppm in the ¹H-NMR spectrum and at δ 74.2 ppm in the ¹³C-NMR spectrum.

The tensile tests were carried out with an Instron 4204 universal testing machine according to ISO 527-1993(E) with the specimen type 1BA. The test speed was 1 mm/min during the first 20% of the elongation (modulus, yield strain, and yield strength), and then it was increased to 10 mm/min (tensile strain and tensile strength). Charpy impact tests were performed with notched specimens according to ISO 179-1993(E). A Zwick 5120 pendulum-type testing machine with a 0.5-2 J hammer was used (specimen dimensions 4 x 6 x 50 mm³, dimensions at the notch 4x 4.8 x50 mm³, notch type A, span 40 mm). Before mechanical testing, the samples were conditioned for at least 48 h (room temperature testing at 23 °C and 50% relative humidity; cold toughness, in a freezer at -20 °C).

SEM (scanning electron microscopy) was used to detect the fracture mechanism and filler/matrix interaction of the composites as well as the possible core-shell structure. The SEM micrographs were taken from the fracture surfaces after the Charpy impact tests. The rubbery phase was removed from the fracture surfaces by etching (leaching) in xylene at ambient temperature for 15 min. The SEM micrographs were run with a JEOL JSM-6335F field emission scanning electron microscope. The fractured

surfaces were sputter-coated with carbon and the electron micrographs were taken using an acceleration voltage of 5 or 15 kV.

WAXS (wide-angle X-ray scattering) was used to determine the crystalline structure of the PP matrix. Owing to the pronounced orientation of the crystalline parts in the tensile test specimens, the WAXS curves were determined from the less oriented impact test specimens (thinned from 4 mm to 2 mm). Samples were measured with a rotating anode Rigaku X-ray generator, with a Cu anode in fine focus (0.3 mm × 3 mm). The beam was focused on the detector and monochromatised using a totally reflecting mirror and a Si (111) monochromator, giving a Cu $K\alpha_1$ beam of size 2 mm × 2 mm on the sample surface. The measurement time per sample was between 10 and 20 min. The distance from the sample to the detector was 135 mm and the magnitude of the scattering vector $q = 4\pi\sin(\theta)/\lambda$ was calibrated using silver behenate and silicon powder. Here θ is half of the scattering angle and λ is 0.15406 m. The range of the magnitude of the scattering vector was from 2 to 30 nm^{-1}. The scattered radiation was detected with an image plate detector MAR345 using a pixel size of 0.15 mm. The intensities were integrated over the azimuth angle and the absorption corrected, the air scattering background was subtracted from the curves, and the intensities were corrected for the flatness of the detector.

RESULTS

Preparation and Characterisation of Copolymers

Ethylene was copolymerised with 1,7-octadiene using a metallocene catalyst in order to achieve unsaturation in the polyethylene chain. Applying information from our previous studies[15,18,19], polymerisation conditions were optimised to obtain a copolymer

with significant amount of diene incorporated in the polyethylene chain but without crosslinking of the product. Copolymerizations were carried out at 80 °C, the ethylene pressure being 500 kPa. The catalyst system *rac*-ethylenebis(indenyl)zirconium dichloride/methylaluminoxane (Et(Ind)$_2$ZrCl$_2$/MAO) was chosen because of its ability to incorporate co-monomer and because it incorporates 1,7-octadiene into polyethylene almost solely as branches, not as cyclic units. The properties of the copolymer (PE-co-diene) are listed in **Table 1**.

Hydrosilylation reactions of PE-*co*-1,7-octadiene copolymer were carried out under extremely dry conditions since the chloro- and ethoxysilane groups are moisture sensitive and this could lead to crosslinking of the copolymer. The hydrosilylation reactions were successfully carried out with dimethylethoxysilane, chlorodimethylsilane, and dimethylphenylsilane as seen in the replacement of the characteristic ^{1}H-NMR shifts of the double bond at the chain end by shifts attributed to the attached silane groups (**Figure 2a** *vs.* **b**, **c**, **d**). These shifts correlated well with the shifts assigned earlier[17].

The properties of the ethylene/diene copolymer changed slightly during the post-treatment (**Table 1**). In the DSC heating curve these changes can be seen as a decrease in the area of

thicker lamellae (**Figure 3a** *vs.* **b**, **c**, **d**). In the GPC curves, the shoulder in the high molar mass part enlarges (**Figure 4a** *vs.* **b**, **c**, **d**) indicating chain extension. This is in accordance with our earlier results[15].

CHARACTERISATION OF THE COMPOSITES

Tensile Properties

The tensile properties of the composites are presented in **Table 2**. As mentioned above, the modulus of the PP/rubber/filler composites is determined by the filler concentration in the PP matrix. Although rigid inorganic fillers increase the stiffness of all polymeric phases, their influence on PP/rubber/filler composites is negligible if the filler particles are located in the soft rubbery phase. As a result, the filler also increases the effective volume fraction of the rubbery phase, which leads to a decrease in the overall stiffness of the composite.

Whether fillers favour the PP or the rubbery phase depends on their rheological properties. Here, the amount of filler embedded was roughly estimated by calculating the theoretical modulus of the composite (**Table 2**; Runs 2, 3, and 4; calculated values in parenthesis[20]). As can be seen, the filler slightly favoured the PP matrix at lower filler loadings (Runs 2 and 3), where the measured values were higher than

Table 1. Properties of PE-based copolymers used as modifiers in hPP/μSi composites

Copolymer	T$_m$ °C	T$_c$ °C	ΔH J/g	M$_w$ g/mol	M$_w$/M$_n$	Functionality mol%
PE-co-diene[a]	118.8	109.1	137	115 600	4.5	1.0
PE-co-SiCl	114.1	108.9	114	150 200	6.5	1.0
PE-co-SiOEt	118.4	108.3	115	152 000	5.8	1.0
PE-co-SiPh	118.6	108.1	111	166 500	5.6	1.0
PE-co-SiF	118.7	109.8	125	157 400	2.7	1.0
PE-co-GMA	103.9	92.3	80	87 000	5.0	~1.6

[a]*Polymerisation conditions: T=80 °C; p(C$_2$H$_4$) 500 kPa; V(toluene)=450 cm^3; n(catalyst)=0.3 μmol; Al/Zr= 15000; p(H$_2$)= 50 kPa; t=20 min*

Figure 2. Characterization (by ¹H NMR) of untreated polyethylene-*co*-1,7-octadiene (a) and polyethylene-*co*-1,7-octadiene after hydrosilylation with dimethylethoxysilane (b), dimethylphenylsilane (c), and chlorodimethylsilane (d)
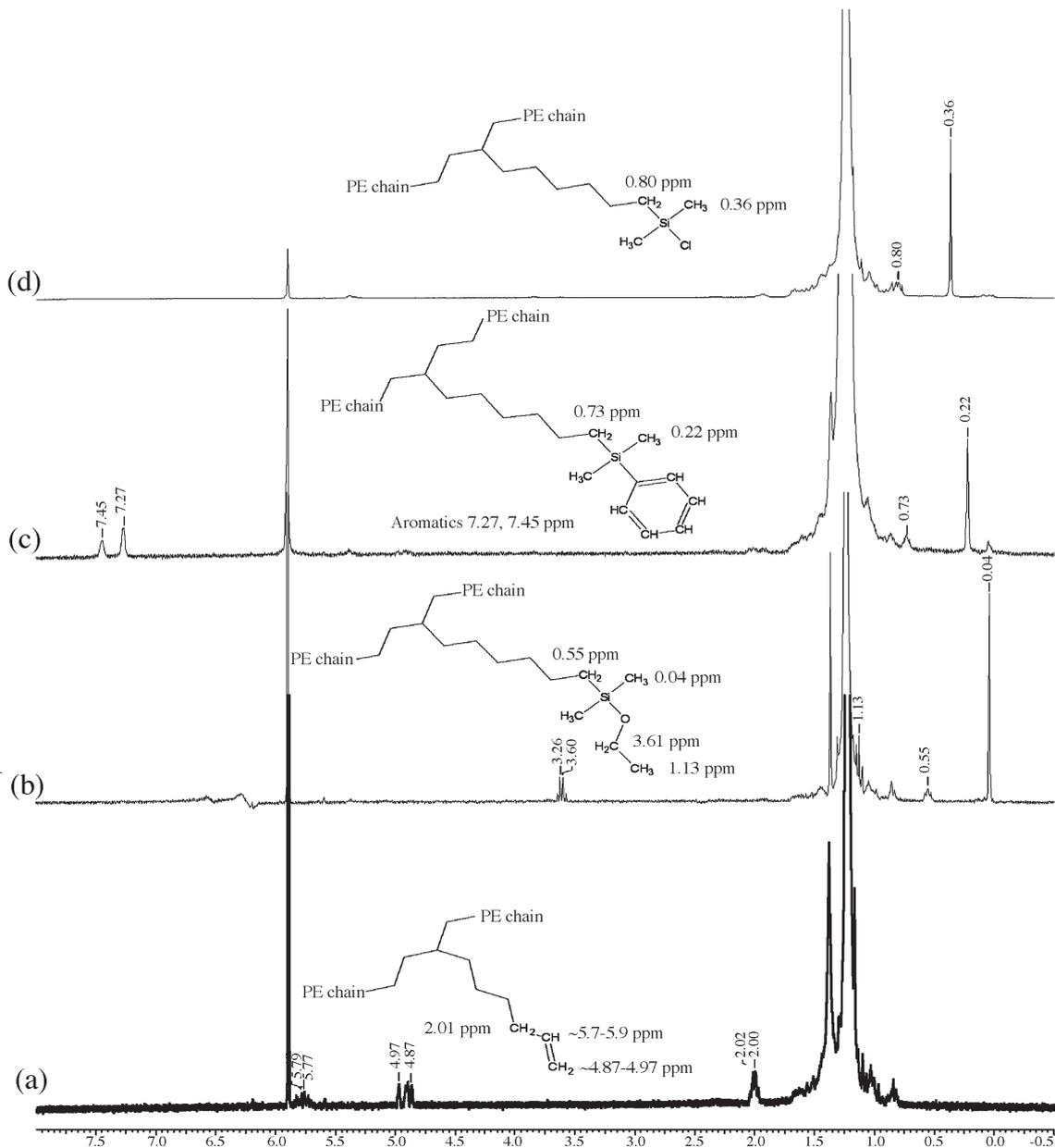
the theoretical ones. In the composite with 30 wt% of μSi (Run 4), the filler particles were dispersed more equally and the calculated value matched well with the observed. These conclusions are only tentative, however, because small errors in the modulus of the hPP strongly influence the calculated values.

Despite the different rheological properties of the PP and rubber phases, the filler dispersion is primarily affected by thermodynamics[6]. This could be seen in the increased modulus when functional PP was used as the modifier (Run 8 vs. Run 4), indicating that the filler concentration in the PP phase was enhanced. The effect was the opposite when functional PEs

were used. As observed earlier in our laboratory, these copolymers dispersed into the rubbery phase (PP-co-PE) rather than into the PP matrix and thereby improved the filler dispersion in the rubbery phase, too[21]. In addition, the stiffening effect of any filler that remained in the PP matrix was expected to decrease after the filler particles were covered with the functional PE. A

Figure 3. DSC curve of untreated PE-*co*-diene (a) and the curves after hydrosilylation to PE-*co*-SiPh (b), PE-*co*-SiOEt (c), and PE-*co*-SiCl (d)
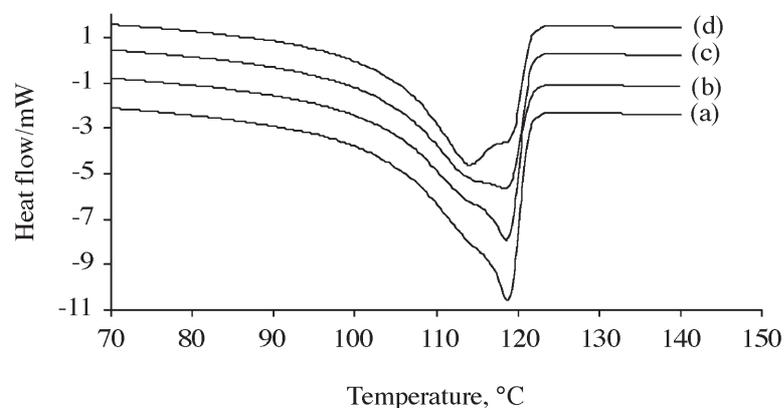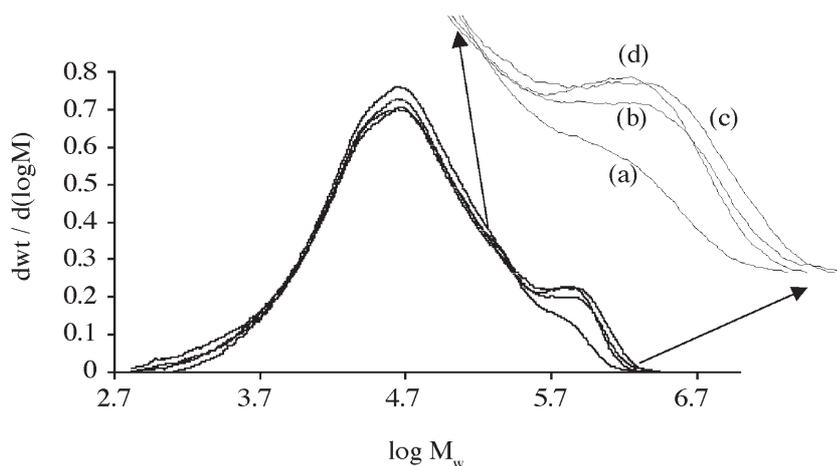

Figure 4. The molar mass distribution of polyethylene-*co*-1,7-octadiene before (a) and after hydrosilylation with HSi(CH$_3$)$_2$Ph (b), HSi(CH$_3$)$_2$OEt (c), and HSi(CH$_3$)$_2$Cl (d)

decrease in the modulus could already be observed with the smaller addition of commercial PE-co-GMA (Run 9 *vs*. Run 4), indicating a considerable change in the morphology of the composite. The softening was more marked with 2 wt% of PE-co-GMA, and the modulus dropped clearly below the value of the unfilled hPP, while the yield strain was more than 40% higher (Run 11 vs. Run 1). This result can be explained by the dispersal of most of the filler in the rubbery phase, which also significantly increased its volume fraction in the composite. Furthermore, the stiffening effect of the filler that remained in the PP matrix seemed to be diminished because the filler particles were covered with the soft PE-co-GMA.

Polyolefins produced with metallocene catalysts differ from polyolefins obtained by conventional technologies. The single-site nature of metallocene catalysts gives rise to products with homogeneous structure and high rigidity. When 0.5 wt% of metallocene-based functionalized polyethylene PE-co-SiX (X=Cl, OEt, F) was added to the composite, the influence on the modulus was negligible (Runs 12, 15 and 18). In experiments where 2 wt% was added, both the modulus and the

yield strain of the composite were influenced (Runs 14, 17, and 20 vs. Run 4), but the undesirable softening effect was not as marked as it was with PE-co-GMA. Like PE-co-GMA, the metallocene-based functional PE-modifiers were able to increase the filler load in the rubbery phase. Their influence on the stiffening effect of the filler in the matrix was noticeably smaller, however, and the decrease in the modulus originated mainly from the reduced filler concentration in the PP matrix.

Besides increasing the modulus, a filler often increases the yield strength of the composite (reinforcing effect). However, several factors determine the level of reinforcement obtained by adding filler, and usually it is considered that spherical particles, like the microsilica in this study, do not reinforce the material[22]. Thus, in our case, the yield strength declined slightly with increases in the filler concentration (from Run 1 to Run 4). The differences in yield strength between the other compositions were small and no conclusions could be drawn.

The tensile strain decreased sharply with filler loading. It was slightly increased when commercial PE-co-GMA was used as modifier and the filler was located mostly in the rubbery phase. The small values of the standard deviations in all the tensile strain results indicate adequate mixing in the preparation of the composite.

Crystalline Properties

Isotactic polypropylene is polymorphic, with the ability to crystallise into several different structures. The most stable form is the monoclinic α-form, even though at least a part of the polymer remains in mesomorphic (or smectic) form. While the nature of the mesomorphic form is not totally understood, it is often described as a structure located between the totally amorphous phase and the thermally

Table 2. Tensile properties of hPP/μSi composites. The values of modulus, yield strain and yield strength are results with draw speed 1 mm/min. The values of tensile strain and tensile strength are results obtained using a draw speed of 10 mm/min. The theoretical modulus values in parenthesis were calculated by the extended Kerner equation[20]

Run	Composite	Modulus MPa	Yield strain %	Yield strength MPa	Tensile strain %	Tensile strength MPa
Run **1**	hPP	770 ± 20	9.9 ± 0.2	25.6 ± 0.2	740 ± 30	34.1 ± 0.3
Run **2**	+ 10 wt-% silica (4.3 vol-%)	880 ± 20 (850)	7.3 ± 0.2	24.3 ± 0.2	530 ± 20	29.0 ± 0.4
Run **3**	+ 20 wt-% silica (9.1 vol-%)	1000 ± 30 (950)	5.5 ± 0.1	23.6 ± 0.3	370 ± 30	25.8 ± 0.2
Run **4**	+ 30 wt-% silica (14.7 vol-%)	1090 ± 30 (1080)	4.6 ± 0.1	23.6 ± 0.2	250 ± 10	25.0 ± 0.3
	hPP+30 wt-% silica					
Run **5**	+ 2.0 wt-% PE-co-diene	1070 ± 20	4.8 ± 0.1	22.9 ± 0.3	250 ± 20	24.7 ± 0.4
Run **6**	+ 2.0 wt-% PE-co-SiPh	1070 ± 20	4.7 ± 0.1	23.0 ± 0.3	260 ± 20	24.2 ± 0.7
Run **7**	+ 2.0 wt-% PP-g-MAH	1090 ± 20	4.8 ± 0.1	23.4 ± 0.3	250 ± 20	23.9 ± 0.6
Run **8**	+ 2.0 wt-% PP-g-COOH	**1140** ± 20	4.7 ± 0.1	23.8 ± 0.3	260 ± 10	24.7 ± 0.5
Run **9**	+ 0.5 wt-% PE-co-GMA	**950** ± 10	**6.9** ± 0.2	23.8 ± 0.3	**280** ± 10	24.4 ± 0.5
Run **11**	+ 2.0 wt-% PE-co-GMA	**710** ± 20	**13.8** ± 0.4	24.9 ± 0.4	**310** ± 10	26.8 ± 0.7
Run **12**	+ 0.5 wt-% PE-co-SiCl	1100 ± 20	4.8 ± 0.1	23.2 ± 0.3	240 ± 20	23.9 ± 0.6
Run **14**	+ 2.0 wt-% PE-co-SiCl	**1010** ± 40	**6.0** ± 0.1	24.4 ± 0.5	230 ± 10	25.4 ± 0.6
Run **15**	+ 0.5 wt-% PE-co-SiOEt	1090 ± 10	**5.2** ± 0.1	23.7 ± 0.3	240 ± 10	24.4 ± 1.2
Run **17**	+ 2.0 wt-% PE-co-SiOEt	**890** ± 30	**7.8** ± 0.1	23.4 ± 0.4	250 ± 20	24.9 ± 0.4
Run **18**	+ 0.5 wt-% PE-co-SiF	1090 ± 50	4.9 ± 0.1	24.1 ± 0.5	230 ± 20	24.8 ± 0.7
Run **20**	+ 2.0 wt-% PE-co-SiF	**960** ± 30	**7.4** ± 0.1	24.2 ± 0.4	260 ± 20	25.7 ± 0.9

stable α-form. The trigonal β-form is rare and requires special crystallisation conditions or the presence of a selective β–nucleating agent. The triclinic γ-form is the least common and is observed only in low molar mass fractions or polymers crystallised under high pressure[23,24,25].

The diffraction maxima due to α- and β-phases of PP are clearly observable in WAXS curves[26]. The intensities of the reflections from α- and β-phases of the different composites were compared and very little variation was found in most cases. Since the samples were slightly oriented, exact determination of the amounts of α- and β-phases was not possible. Notable differences were observed only between unfilled hPP,

hPP/μSi composite, and the hPP/μSi composites with 2 wt% of functional PE (**Figure 5a**, **b**, **c**). The PP phase of the unfilled hPP consisted primarily of the α-crystalline form, with only a small amount in β-crystalline form (seen at reflection 300). The formation of this trigonal structure is highly sensitive to the prevailing conditions and it appears that the presence of microsilica in the PP matrix disturbs its formation. However, the proportion of the β-crystalline form was greater in the composite containing 2 wt% of functional PE (PE-co-SiOEt, PE-*co*-GMA, PE-co-SiF) than in the unfilled hPP.

Thermal properties of the composites are presented in **Table 3**, and the DSC

heating curves of selected composites in **Figure 6**. The curves are dominated by the melting endotherm of the α-crystalline PP matrix, since the rubbery phase is amorphous. The melting temperature (T_m) of the PP matrix was 163.7 °C, and it increased by about 1 °C when silica was added to the matrix (**Figure 6a** *vs*. **b**). Furthermore, the use of any modifier in the composite had only a moderate influence on the melting temperature. A small shoulder in the DSC heating curve was detected at about 150 °C, which is the typical melting temperature for the trigonal β-crystalline structure of PP. In the curve of the composite with 2 wt% of PE-co-SiOEt (**Figure 6d**), the shoulder was more like a distinct peak.

Figure 5. WAXS spectra of unfilled hPP (a), hPP/μSi composite (b), and hPP/*μ***Si composite with 2 wt% of PE-*co*-SiOEt (c)**
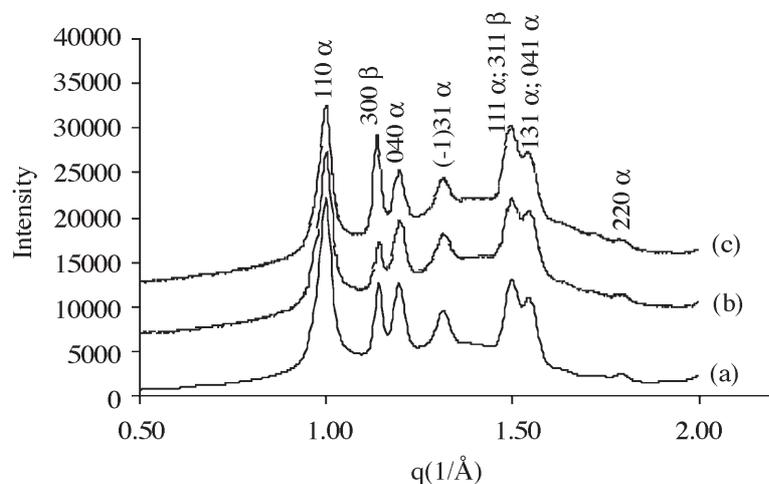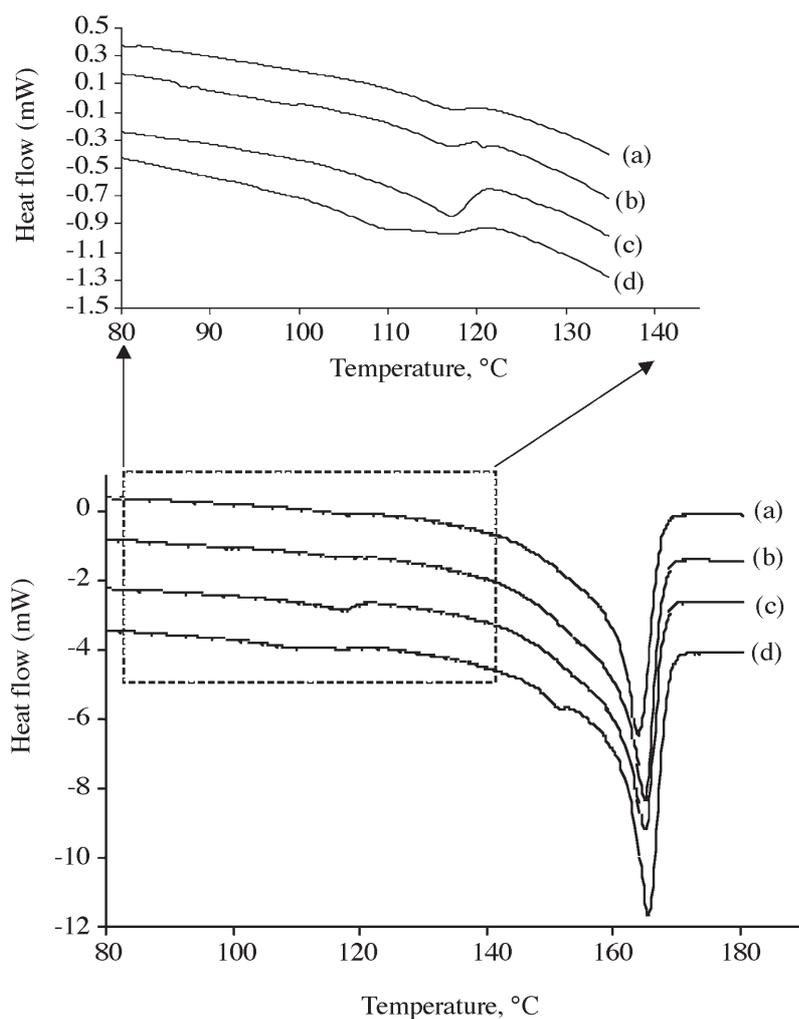

Figure 6. DSC curve of hPP (a) and the curves of composites hPP/μSi (b), hPP/μSi + 2 wt% of PE-*co*-SiF (c), and hPP/μSi + 2 wt% of PE-*co*-SiOEt (d). The curves are shifted along the y-axis for clarity

An additional endothermic peak, at 115-120 °C, can be seen in the magnification of the DSC curves (**Figure 6**, inset). This peak is due to the small homopolyethylene fraction formed during polymerisation of the hPP. For composites containing our PE-based modifiers (**Figure 6c** and **d**), the area of the peak is increased notably. Clearly at least part of the copolymer was able to form a characteristic crystalline structure (**Figure 3**, **Table 1**, melting at 114-119 °C). This structure must have originated from modifier located in the rubbery phase since free crystallisation of the copolymer at the filler/matrix interphase would be prohibited by the strongly crystallised solid PP matrix. Unfortunately, the signal from the mesomorphic form of the PP matrix made it impossible to characterise this small peak accurately. The mesomorphic form is stable at room temperature, but it transforms to the monoclinic α-form during heating, starting at 40 °C[27]. It is seen in the DSC curve as a broad exothermic peak, which disturbed the detection of the crystalline region at 100-120 °C.

The addition of filler had a significant influence on the crystallisation temperature (T_c) of the PP matrix. As expected, the silica particles located in the PP matrix behaved as nucleating agents and the crystallisation temperature of the PP matrix was increased (**Table 3**, Run 1 *vs.* Runs 2, 3, and 4). Although monitoring of the crystallisation temperature can give information on the filler concentration in the PP matrix, the correlation is clear only at low filler loadings of 0-10 vol%[20]. In our case there was no correlation between filler loading and T_c in composites having a microsilica concentration greater than 20 wt% (9.1 vol%). At the higher concentration, only distinct variations in filler dispersion due to modifiers were reflected as changes in the crystallisation temperature.

The crystallisation temperature was more heavily influenced by the

Table 3. Thermal characterization of hPP and hPP/μSi composites with and without modifiers

Run	Composite	T_m °C	T_c °C	ΔH J
Run 1	hPP	163.7	123.1	80.3
Run 2	+10 wt-% silica	164.1	125.5	80.8
Run 3	+20 wt-% silica	164.7	126.0	83.9
Run 4	+30 wt-% silica	164.8	**125.8**	86.5
	hPP+30 wt-% silica			
Run 5	+ 2.0 wt-% PE-co-diene	164.8	126.1	87.0
Run 6	+ 2.0 wt-% PE-co-SiPh	164.8	125.6	86.8
Run 7	+ 2.0 wt-% PP-g-MAH	164.8	126.4	84.4
Run 8	+ 2.0 wt-% PP-g-COOH	164.9	126.5	86.4
Run 9	+ 0.5 wt-% PE-co-GMA	164.2	125.0	85.3
Run 11	+ 2.0 wt-% PE-co-GMA	164.5	124.8	84.0
Run 12	+ 0.5 wt-% PE-co-SiCl	164.8	125.9	85.9
Run 14	+ 2.0 wt-% PE-co-SiCl	165.0	125.9	82.2
Run 15	+ 0.5 wt-% PE-co- SiOEt	164.8	125.9	86.0
Run 17	+ 2.0 wt-% PE-co-SiOEt	165.3	125.6	83.7
Run 18	+ 0.5 wt-% PE-co-SiF	164.8	125.9	83.0
Run 20	+ 2.0 wt-% PE-co-SiF	164.8	125.6	84.7

Table 4. Toughness of hPP and hPP/ μSi composites (with and without modifiers) above and below the T_g of PP. Impact strength values are for notched specimens. The strengths of composites injection molded at of 80 °C rather than the normal 40 ºC are presented in parenthesis

Run	Composite	Impact strength	
		at 25 °C kJ/m²	at - 20 °C kJ/m²
Run 1	hPP	11.6 ±1.6 (11.7 ± 0.8)	6.0 ± 0.4 (5.9 ± 1.0)
Run 2	+ 10 wt-% silica	20.3 ± **9.2**	-
Run 3	+ 20 wt-% silica	29.8 ± **9.9**	-
Run 4	+ 30 wt-% silica	**38.4** ± 4.1 (**15.6 ± 3.4**)	4.6 ± 0.2 (4.6 ± 0.8)
	hPP + 30 wt-% silica		
Run 5	+ 2.0 wt-% PE-co-diene	**38.8** ± 1.9	4.6 ± 0.3
Run 6	+ 2.0 wt-% PE-co-SiPh	**38.0** ± 2.5	4.6 ± 0.5
Run 7	+ 2.0 wt-% PP-g-MAH	19.7 ± **10.2**	3.4 ± 0.3
Run 8	+ 2.0 wt-% PP-g-COOH	10.0 ± 1.1	2.8 ± 0.1
Run 9	+ 0.5 wt-% PE-co-GMA	10.7 ± 0.8	6.0 ± 0.5
Run 10	+ 1.0 wt-% PE-co-GMA	**15.2** ± 0.4	**6.4** ± 0.4
Run 11	+ 2.0 wt-% PE-co-GMA	**20.6** ± 0.8	**7.7** ± 0.6
Run 12	+ 0.5 wt-% PE-co-SiCl	30.8 ± **7.7**	4.7 ± 0.4
Run 13	+ 1.0 wt-% PE-co-SiCl	11.6 ± 2.5	4.0 ± 0.4
Run 14	+ 2.0 wt-% PE-co-SiCl	11.4 ± 2.2	3.7 ± 0.3
Run 15	+ 0.5 wt-% PE-co-SiOEt	22.8 ± **9.3**	4.1 ± 0.4
Run 16	+ 1.0 wt-% PE-co-SiOEt	10.2 ± 0.9	4.8 ± 0.3
Run 17	+ 2.0 wt-% PE-co-SiOEt	**15.5** ± 2.2	**7.1** ± 0.3
Run 18	+ 0.5 wt-% PE-co-SiF	14.4 ± **9.0**	3.4 ± 0.4
Run 19	+ 1.0 wt-% PE-co-SiF	10.1 ± 0.5	4.8 ± 0.2
Run 20	+ 2.0 wt-% PE-co-SiF	**17.8** ± 3.7	**7.4** ± 0.7

functional modifiers because they changed the interaction between the filler and the matrix. Compared with the original hPP/μSi composite, T_c was raised (slightly, but clearly) when PP-based modifier was used in the composite (Run 4 *vs.* Runs 7 and 8). The functionalized PP bonded the filler more tightly to the PP matrix, resulting in a more effective nucleation. Addition of the PE-based modifier PE-co-GMA clearly depressed the T_c (Run 4 vs. Run 9 and 11), owing to the reduced filler loading in the PP matrix (but also to the poorer nucleation ability of the fillers remaining in the matrix). This result was in good accord with the tensile properties, indicating extensive modification of the composite morphology. In contrast to the case of PE-*co*-GMA, the crystallisation temperature was little affected when the metallocene-based polyethylenes were used as modifiers (Run 4 vs. Runs 12, 14, 15, 17, 18, and 20) even though they reacted with the filler influencing the morphology of the composite. The ability of the filler to act as a nucleating agent was not reduced after its reaction with metallocene-based functional PE.

Toughness vs. Morphology

The results of toughness tests of the composites are presented in **Table 4**. Since all the unnotched samples remained unbroken at ambient temperature, toughness was evaluated with notched samples. Unexpectedly, the addition of microsilica particles increased the toughness of the hPP/μSi composite (Run 1 *vs.* Runs 2, 3, and 4). In the case of 10 and 20 wt% of microsilica, the test specimens fractured partly in a brittle manner and partly in a ductile manner (characteristic impact strengths ~8-15 kJ/m² and ~30-45 kJ/m², respectively), and standard deviations were large. Finally, with 30 wt% of microsilica added to hPP (Run 4), all the test specimens fractured in ductile manner and the notched impact strength was increased by over 200% compared with the unfilled hPP.
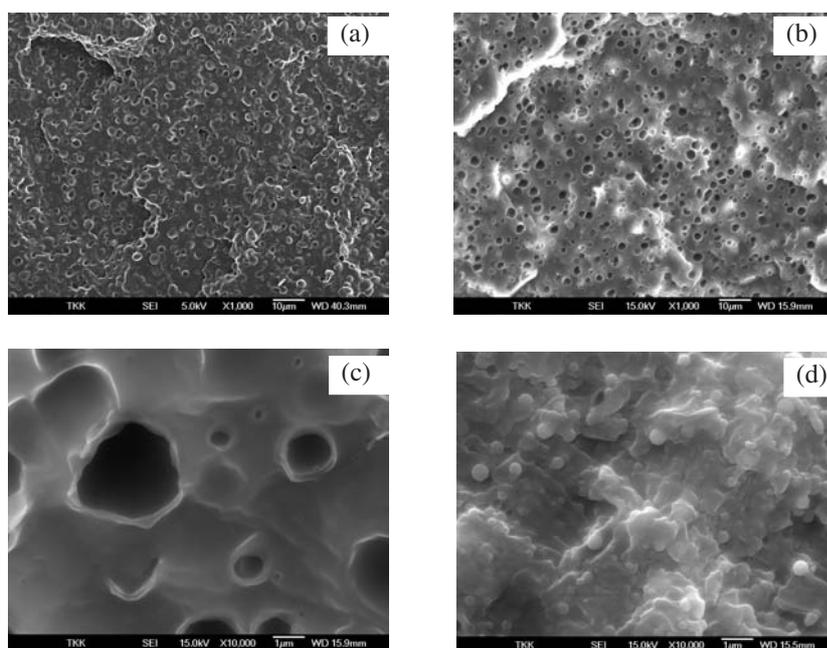
According to the SEM micrographs, the fracture mechanism was totally different in the brittle fracture of hPP and the ductile fracture of hPP/μSi composites. The rubbery particles at the fracture surface of unfilled hPP (**Figure 7a**) were seen as round blisters (rubber particles, diameter ~3 μm) and craters (where rubber particles had been detached from the matrix). This interpretation was confirmed by dissolving the rubbery particles in xylene and observing the replacement of the blisters with craters (**Figure 7a** *vs.* **b**). Higher magnification

(**Figure 7c**) showed that the fracture surface between the rubber particles was smooth. The crack seemed to proceed linearly in the PP matrix before striking the rubber particles, and then continued by winding around them *via* the rubber/matrix interphase (**Scheme 1a**).
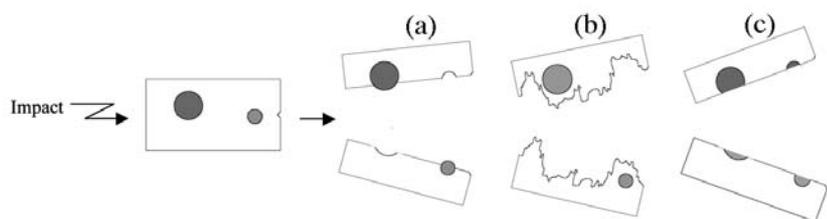
In contrast to unfilled hPP, no rubbery phases in the form of blisters and craters were detected at the fracture surface of the hPP/μSi composite (**Figure 8a**). No clear craters were seen even after xylene leaching

(**Figures 8b** and **7d**), indicating that the fracture proceeded mainly in the PP matrix, avoiding the rubber and the rubber/matrix interphase. Another difference in the fracture mechanisms was evident at higher magnification. In the hPP/μSi composites the fracture surface was rougher (**Figure 7d** *vs.* **c**) as the crack proceeded more randomly, taking a longer route through the PP matrix (**Scheme 1b**). With the rubbery particles in the hPP/μSi composite no longer fully participating in the toughening mechanism, the ductile fracture of the hPP/μSi composite was probably due to the significantly larger fracture area.

The ductile fracture mechanism was not stable and a slight increase in the moulding temperature (**Table 4**, Run 4, values in parenthesis) or the addition of functional polyolefin (Runs 7, 12, 15, 18) caused the fracture mechanism to move towards the brittle mode. Neither 0.5 wt% of metallocene based functional polyethylene nor 2 wt% commercial MAH functionalized PP was sufficient to change the fracture mechanism of the composites completely, and the test specimens were not fractured uniformly but were partly brittle and partly ductile (with large standard deviations). The mechanism of fracture was fully brittle in the case of 0.5 wt% of PE-co-GMA and 1 wt% of our functionalized PEs (Runs 9, 13, 16, 19). The same was true for an increase in the total functionality of the PP-based modifier (Run 8 *vs.* Run 7). The impact resistance of these composites was at the level of the unfilled hPP. This could also be seen in the SEM micrographs, where the fracture surface resembled that observed for unfilled hPP (**Figure 8c** and **d** *vs.* **Figure 7a** and **b**, note the difference in the magnification).

Surprisingly, an increase in the amount of functionalized polyethylene in the hPP/μSi composite to 1 wt% (Run 10) or 2 wt% (Runs 11, 17, and 20) caused an increase in the impact strength. Now the fracture mechanism

Figure 7. SEM micrographs of the fracture fields of samples fractured at ambient temperature. hPP (*1000) (a), xylene leached hPP (*1000) (b), (*10 000) (c), and xylene leached hPP/μSi composite (*10 000) (d)


Scheme 1. Schematic presentation of the crack propagation in brittle (a), ductile (b), and semibrittle (c) fracture mechanisms. Top view, the notch is on the right side and the impact comes from the left. The rubbery phase is gridded. The filler particles are removed for clarity

Figure 8. SEM micrographs (*2500) of the fracture fields of composite samples fractured at ambient temperature. hPP/μSi before (a) and after (b) xylene leaching and hPP/μSi + 2 wt% of PP-*g*-COOH before (c) and after (d) xylene leaching
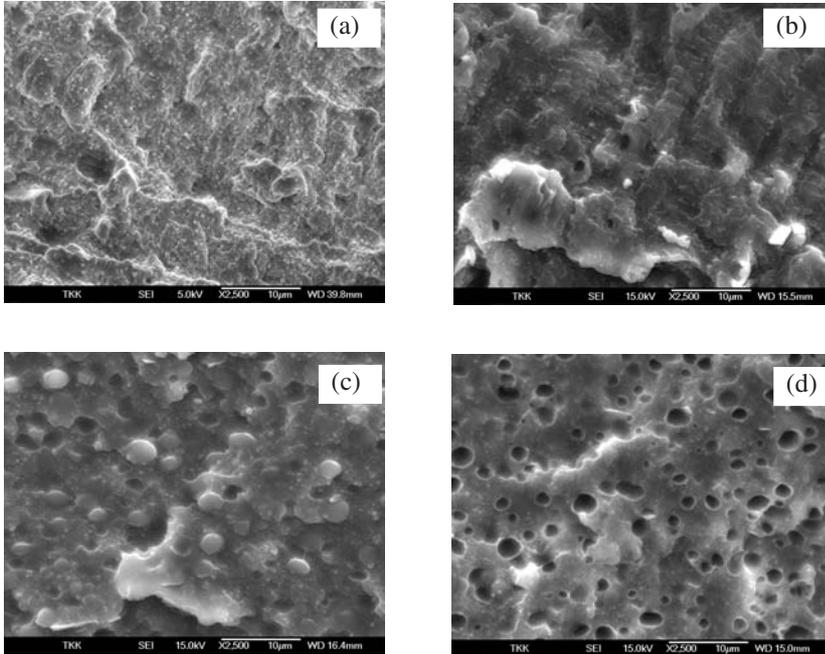
seemed to be somewhere between the ductile and brittle mechanisms. The blisters, or craters formed from the detached rubbery particles, were barely detectable in the SEM-micrographs (**Figure 9a, c**), suggesting a ductile fracture mechanism (**Figure 8a**). However, craters were formed at the fracture surfaces when the rubber particles were leached with xylene (**Figure 9b, d**). The number of craters was less than in the corresponding SEM micrographs of brittle fractures (**Figures 7b** and **8d**), but that was due to the large amount of filler embedded in the rubbery phase (**Figure 9e**). With the higher magnification (**Figure 9e**) a smooth fracture surface could be seen between the rubbery particles, which is consistent with the brittle fracture mechanism. However, the crack was now able to pass through the rubber particles (**Scheme 1c**) rather than to wind around via the rubber/matrix interphase as in the brittle fracture (**Scheme 1a**). The ability of the rubbery

Figure 9. The SEM micrographs (*2500) of the fracture fields of composite samples fractured at ambient temperature. hPP/μSi + 2 wt% of PE-*co*-SiOEt before (a) and after (b) xylene leaching; hPP/μSi + 2 wt% of PE-*co*-GMA before (c) and after (d) xylene leaching. e) as d but *10 000
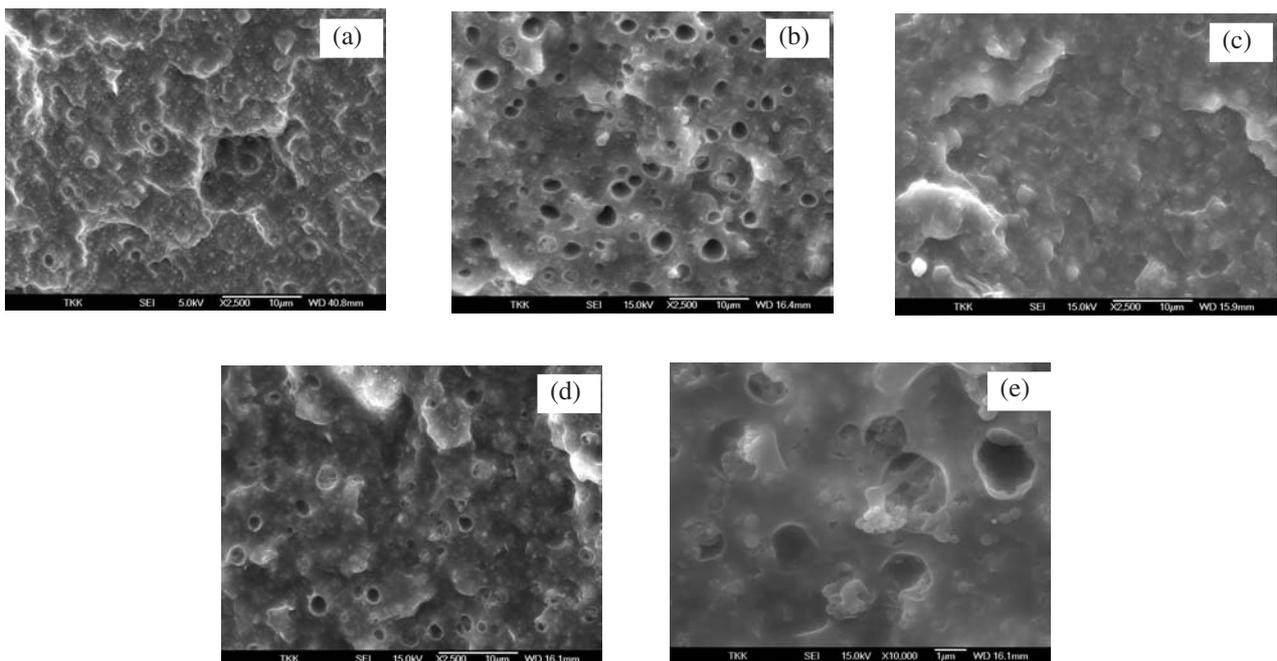
phase to carry a larger amount of the impact energy than the rubber/matrix interphase was being utilised in this "semi-brittle" mechanism.

PP is more brittle below its T_g because its capacity for shear yielding becomes negligible, and crazing dominates during the fracture. In our study, this was clearly seen as the drop in toughness of hPP took place from 11.6 kJ/m^2 at 25 °C to 6.0 kJ/m^2 at -20 °C (**Table 4**, Run 1). A more significant change in toughness took place in the hPP/μSi composite (Run 4), where the impact strength decreased from 38.8 to 4.6 kJ/m^2. In the SEM micrographs it could be seen that hPP/μSi fractured in a ductile manner at ambient temperature, but in a brittle manner at lower temperature.

At ambient temperature, an increase in the concentration of functionalized polyethylene in the composite from 0.5-1 wt% to 1-2 wt% changed the fracture from brittle to semi-brittle and the toughness of the composite increased. The same trend was seen at the lower temperature (Runs 10, 11, 17, 20); the semi-brittle fracture mechanism also dominated for these composites at -20 °C. The glass transition temperature of the rubbery phase was noticeably lower than -20 °C so that the material was still able to consume large quantities of impact energy.

DISCUSSION

The increase in impact resistance after addition of submicron-size filler particles (<1 μm) to the PP matrix is usually explained by the separation of the filler from the matrix. Instead of crazing, the small cavities that form allow shear yielding to take place, after which the voids act like rubber particles and the fracture mechanism changes from brittle to ductile. On this explanation, the increase in toughness would be lost if the shear yielding or the debonding were prevented.

The results of our studies support the above explanation only in part. Support is provided by three observations. First, the toughness correlated with the increasing filler concentration in the matrix, as could be expected since the amount of voids that formed would have increased. Secondly, no increase in toughness of the hPP/μSi composite was seen at temperatures below the T_g of PP, since the capability of the matrix for shear yielding is reduced at lower temperatures where crazing was dominant. Thirdly, the PP based functionalized modifiers were able to bind the filler stronger to the matrix (higher T_c) and thereby hinder debonding, and decrease the toughness of the composite.

On the other hand, the yield strength of the composite should have increased when functionalized PP was used to bind the filler to the matrix. In the case of our modifiers, the increase was decidedly moderate. Prevention of the debonding would have required more than 2 wt% of the modifier. Moreover, functionalized PE would not in general be expected to bind the filler to the matrix in hPP/μSi composites because of the immiscibility of PP and PE. Also, the change in the mould temperature (from 40 °C to 80 °C) in the injection moulding of hPP/μSi composite could not have had such a detrimental influence if the debonding mechanism were prevailing. Finally, no signs of the microstructures that should form after filler debonding were found in our SEM micrographs. Evidently the increase in toughness of the hPP/μSi composite relative to hPP resulted from the ability of the filler to control the growth path of the crack, which finally led to a notably larger fracture surface and a more ductile fracture compared with the unfilled hPP.

Although the reason for the ductile fracture mechanism and its sensitivity remains unclear, there seems to be a connection with the transcrystalline phase of PP formed at the PP/filler interphase or at the filler surface.

Usually such a transcrystalline phase is considered weak and rigid, leading to decreased overall toughness[1]. In our case, however, the reverse seemed to be the case. The formation of this transcrystalline phase is clearly sensitive to the conditions. It could easily be disturbed by the presence of functionalized polyolefin at the filler surface, or by a change in the cooling or crystallisation rate. This could happen through, for example, a change in the mould temperature.

The use of untreated PE-co-diene and weakly interacting PE-co-SiPh had practically no influence on the mechanical properties of hPP/μSi composite (**Tables 2** and **4**, Runs 5 and 6). Clearly these modifiers were unable to interact strongly enough with the filler to influence the morphology or the filler/matrix interaction. PE-co-SiCl had only moderate influence on the composite (**Tables 2** and **4**, Runs 12-14), though it was expected to be more reactive than the other silane groups used in this study. One explanation is its preference to react with itself rather than with the filler. Halo- and alkoxysilane groups are unable to react directly with the hydroxyl groups of the inorganic filler; they require a catalytic amount of water to change the PE-SiX group to PE-SiOH, which is able to form a covalent bond with the metal-OH[28]. As a competing reaction, the PE-SiOH groups react with themselves, resulting in a crosslinked structure (PE-Si**X**→PE-SiOH→PE-SiOSi-PE). This crosslinking reaction is catalysed by HCl, which is a side product in the reaction between PE-*co*-SiCl and H$_2$O.

The other polyethylene-based modifiers that were studied (PE-co-SiF, PE-co-SiOEt, PE-co-GMA) reacted with the microsilica filler, and the filler particles were effectively dispersed in the rubbery phase. A large concentration of filler particles in the rubbery phase fulfils the requirement for a semi-brittle fracture mechanism. Unlike the ductile fracture mechanism, the semi-brittle

one is maintained at -20 ℃, and the toughness of the composite was higher than that of hPP. Commercial PE-co-GMA increased the toughness most, but it also resulted in loss of the stiffness achieved by the addition of μSi. When PE-*co*-SiOEt or PE-*co*-SiF was the modifier, almost the same increase in toughness was achieved as with the commercial PE-*co*-GMA, but now with only a moderate decrease in the stiffness (e.g. Run 11 vs. Run 20). This can be explained by the more controlled and rigid structure of polyethylenes made with metallocenes. After reaction of the modifier with the filler, the ability of the filler to act as a nucleating and stiffening agent was largely maintained.

CONCLUSIONS

Many functionalities are difficult if not impossible to insert into polyolefins in co-ordination catalysed polymerisations. Post-functionalisation of olefin/diene copolymers polymerised with metallocene catalysts offers an alternative route to functionalized polyolefins. Facile routes exist, for example, for the hydrosilylation of ethylene/1,7-octadiene copolymers to polyethylenes containing reactive silane functionalities (-SiCl, -SiOEt). Functionalized polyolefins are applied as effective modifiers for polyolefin-based composites and blends. Just 0.5-2 wt% of copolymer containing 1 mol% of functional group effected notable changes in the properties of hPP/μSi composites. The functionalized polyethylenes were able to interact with the filler and transfer part of the filler to the rubbery phase of heterophasic polypropylene. This proved an effective way to guide a propagating crack into the rubbery phase instead of its going around *via* the PP matrix/rubber interlayer. Since the rubbery phase is able to carry more impact energy than the PP matrix/rubber interlayer, a significant improvement was achieved in the toughness compared with that of unfilled hPP, below the T_g of PP as well as at ambient temperature. Even though

part of the functionalized PE-covered filler remained in the PP phase, owing to the rigidity of PE produced with metallocene catalysts, the undesirable softening of the composite was noticeably reduced.

Increased stiffness of heterophasic polypropylene without loss of toughness can be achieved by blending in submicron-size silica fillers. The toughness is lost at temperatures below T_g of PP, however. One way to maintain the toughness at lower temperatures is to use functionalized PE as modifier. Functionalized PE changes the morphology and, in that way, the fracture mechanism of the hPP/μSi composite. The softer nature of PE-based modifiers compared with the PP matrix leads to decreased stiffness, but the softening can be minimised by using the more "rigid" and homogeneous PE grades produced with metallocene catalysts.

REFERENCES

1. Zuiderduin W.C.J., Westzaan C. and Huétink J., *Polymer*, 44 (2003) 261-275.

2. Kaempfer D., Thomann R. and Müllhaupt R., *Polymer*, 43 (2002) 2909-2916.

3. Hornsby P.R. and Premphet K., *J. App. Polym. Sci.*, 70 (1998) 587-597.

4. Liang J.Z., Li R.K.Y. and Tjong S.C., *Polym. Comp.*, 20 (1999) 413-422.

5. Stricker F. and Mülhaupt, R., *J. App. Polym. Sci.*, **62** (1996) 1799-1806.

6. Molnár S.Z., Pukánzky B., Hammer C.O. and Maurer F.H.J., *Polymer*, **41** (2000) 1529-1539.

7. Chan C-M., Wu J., Li J-X. and Cheung Y-K., *Polymer*, **43** (2002) 2981-2992.

8. Thio Y.S., Argon A.S. and Cohen R.E., *Polymer*, **45** (2004) 3139-3147.

9. Qiu G-X., Raue F. and Ehrenstein G.W., *J. App. Polym. Sci.*, **83** (2002) 3029-3035.

10. Bartczak Z., Argon A.S., Cohen R.E. and Weinberg M., *Polymer*, **40** (1999) 2331-2346.

11. Löfgren B., Seppälä J.V., in Scheirs

J. and Kaminsky W., *Metallocene-based polyolefins*, John Wiley and Sons Ltd, Vol 2, (2000), 134-157.

12. Song F., Pappalardo D., Johnson A.F., Rieger B. and Bochmann M., *J. Polym. Sci. Part A: Polym. Chem.*, **40** (2002) 1484-1497.

13. Kaminsky W. and Drögermuller H., *Makromol. Chem. Rapid. Commun.*, **11** (1990) 89-94.

14. Yu Z., Marques M., Rausch M.D. and Chien J.C.W., *J. Polym. Sci. Part A: Polym. Chem.*, **33** (1995) 979-987.

15. Pietikäinen P., Väänänen T. and Seppälä J.V., *Eur. Polym. J.*, **35** (1999) 1047-1055.

16. Naga N., Shiono T. and Ikeda T., *Macromolecules*, **32** (1999) 1348-1355.

17. Lipponen S. and Seppälä J.V., *J. Pol. Sci. Part A: Polym. Chem.*, **42** (2004) 1461-1467.

18. Pietikäinen P., Seppälä J.V., Ahjopalo L. and Pietilä L-O., *Eur. Polym. J.*, **36** (2000) 183-192.

19. Kokko E., Pietikäinen P., Koivunen J. and Seppälä J.V., *J. Polym. Sci. Part A: Polym. Chem.*, **39** (2001) 3805-3817.

20. Stricker F., Bruch M. and Mülhaupt R., *Polymer*, **38** (1997) 5347-5353.

21. Uotila R., Hippi U., Paavola S. and Seppälä J., *Polymer*, **46** (2005) 7923-7930.

22. Rothon, R.N., *Particulate-Filled Polymer Composites*, Rapra Technology, Shawbury, UK, 2nd edition, (2003), 357-424.

23. Bond E.B., Spruiell J.E. and Lin J.S., *J. Polym. Sci. Part B: Polym. Phys.*, **37** (1999) 3050-3064.

24. Varga J., Mudra I. and Ehrenstein W., *J. Therm. Anal. Cal.*, **56** (1999) 1047-1057.

25. Vittoria V., Olley R.H. and Bassett D.C., *Colloid. Polym. Sci.*, **267** (1989) 661-667.

26. Turner-Jones A., Aizlewood J.M. and Beckett D.R., *Die Macromol. Chem.*, **75** (1964) 134-158.

27. Hideki M. and Kenjiro S., *J. Polym. Sci. Part B: Polym. Phys.*, **24** (1986) 2379-2401.

28. Lipponen S. and Seppälä J.V., *J. Polym. Sci. Part A: Polym. Chem.*, **43** (2005) 5597-5608.